Picosecond X-Ray Studies of Coherent Folded Acoustic Phonons in a Multiple Quantum Well

P. Sondhauss,[1,*] J. Larsson,[1] M. Harbst,[1] G. A. Naylor,[2] A. Plech,[2,†] K. Scheidt,[2] O. Synnergren,[3,1] M. Wulff,[2] and J. S. Wark[4]

[1]*Department of Physics, Lund University, P.O. Box 118, SE-221 00 Lund, Sweden*
[2]*ESRF, BP 220, 38043 Grenoble Cedex 9, France*
[3]*School of Technology and Society, Malmö University, S-205 06, Malmö, Sweden*
[4]*Department of Physics, Clarendon Laboratory, University of Oxford, Oxford OX1 3PU, United Kingdom*

(Received 18 January 2005; published 1 April 2005)

Coherent folded acoustic phonons in a multilayered GaSb/InAs epitaxial heterostructure were generated by femtosecond laser pulses and studied by means of ultrafast x-ray diffraction. Coherent phonons excited simultaneously in the fundamental acoustic branch and the first back-folded branch were detected. This represents the first clear evidence for phonon branch folding based directly on the atomic motion to which x-ray diffraction is sensitive. From a comparison of the measured phonon-modulated x-ray reflectivity with simulations, evidence was found for a reduction of the laser penetration depth. This reduction can be explained by the self-modulation of the refractive index due to photogenerated free carriers.

DOI: 10.1103/PhysRevLett.94.125509 PACS numbers: 63.20.Dj, 61.10.-i, 63.20.Kr, 68.65.Fg

Periodic layered semiconductor heterostructures consisting of two or more semiconductor materials in alternating lattice matched thin layers such as multiple quantum wells (MQWs), or superlattices play an important role in modern optoelectronics. Light emitters, diode lasers, and many kinds of photodetectors are based on these heterostructures. Apart from their technological importance, nanometer-scale semiconductor heterostructures are promising candidates for the realization of ''coherent control'' in condensed matter [1–3]. In both cases, it is vital to understand and to be able to control phonons, since phonon-electron interaction in semiconductors is strong. Specific to phonons in periodic layered heterostructures is the effect of branch folding. It can be put down to the destruction of the lattice periodicity along the translation vector of the layer periodicity. As a consequence, the lattice periodicity given by the lattice constant a must be replaced by the heterostructure periodicity D and thus the dimension of the first Brillouin zone (BZ) in this direction reduces dramatically from $2\pi/a$ to $2\pi/D$. The phonon branches have to be folded back into this reduced BZ while small alterations occur in the proximity of the zone boundaries [4], leading to gaps in the frequency spectrum. The folding creates new phonon branches, which lie in frequency between those of the acoustic and the optical branches. Such folded acoustic phonons have been extensively studied by optical techniques [5–9].

Here we present the first clear evidence for folded coherent acoustic phonons in a multiple quantum well by means of time-resolved x-ray diffraction (TRXD). The phonon-related coherent atomic motion indicates a reduction of the laser penetration depth due to the self-modulation of the refractive index by photogenerated free carriers. This effect was observable because ambipolar diffusion, which usually extends the effective penetration depth, was strongly inhibited by the broken-gap lineup of the GaSb/InAs heterojunction.

In the way TRXD was used here, x-ray scattering from phonons is the underlying effect: the phonon-related atomic motion modulates periodically the phases of the scattered x rays. This leads to sidebands of the rocking curve oscillating at the phonon frequency [10–15]. The distance of these sidebands to the center of the rocking curve is directly proportional to the modulus of the phonon wave vector q. Thus by measuring the reflectivity at a certain point on the rocking curve, one probes a single phonon wave vector, provided that the wave vectors of the coherently excited modes are parallel; i.e., the strain profile is one dimensional.

The heterostructure used in the experiment consisted of five GaSb/InAs double layers with single layer thicknesses of 52 and 82 nm, respectively. The layers were grown in the [001] direction by metal-organic vapor phase epitaxy (MOVPE) onto a GaSb substrate. The heterostructure was tested by atomic force microscopy (AFM) and x-ray diffractometry. The AFM scan showed atomic terraces on the GaSb top layer, indicating a good crystal quality. X-ray diffractometry revealed layer thicknesses and misfit strain. The static strain due to a small difference in the lattice constants of InAs and GaSb, $\eta_{\mathrm{mf}} = 0.62\%$, was partially relaxed in the thicker InAs layers which led to a small amount of misfit strain in the GaSb layers as well [16].

The experiment was carried out at beam line ID9 of the ESRF electron synchrotron storage ring in Grenoble. The general setup was very similar to that of previous time-resolved x-ray diffraction measurements, and a more detailed description can be found elsewhere [14]. Coherent acoustic phonons were generated by illuminating the heterostructure with ultrashort laser pulses from a Ti:Al_2O_3-based laser system ($\lambda = 800$ nm, $\tau = 150$ fs),

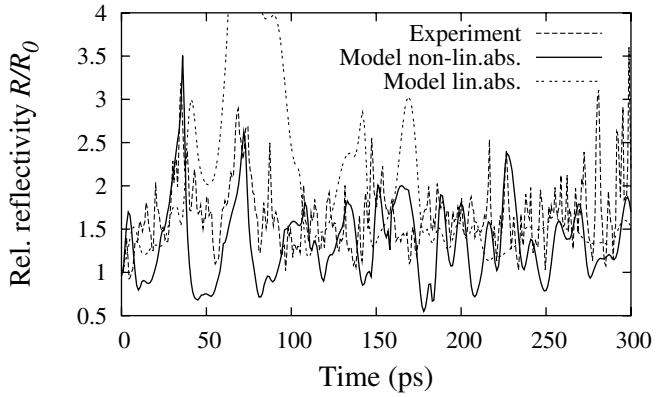

FIG. 1. Evolution of normalized reflectivity at $\theta = \theta_{\text{Bragg}} + 0.61$ mrad.

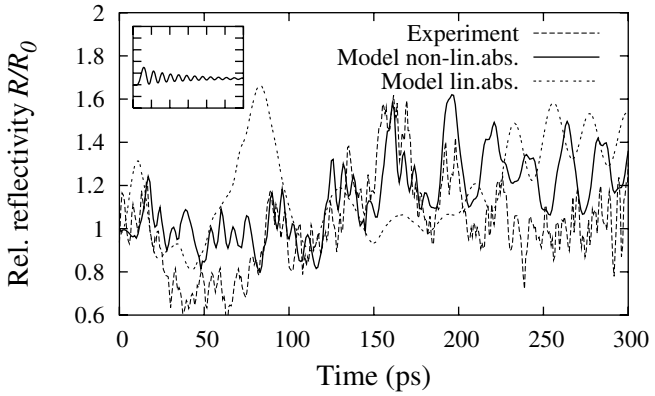

FIG. 2. Evolution of the normalized reflectivity at $\theta = \theta_{\text{Bragg}} - 0.3$ mrad. The inset shows the evolution of the normalized reflectivity at the same angle for a bulk GaSb crystal.

which were incident on the GaSb cap layer at about the Brewster angle ($\varphi = 74\,^\circ$, $\varphi_{\text{Brew}} = 77.3\,^\circ$). The laser was focused down to a spot size of 1.3×0.3 mm^2 on the sample resulting in a fluence at the surface of 8 mJ/cm^2. Since the spot size is large compared to the laser penetration depth, the laser generated strain profile is essentially one dimensional. X rays delivered by the U20 undulator with a divergence of approximately 10 μrad, monochromatized to 16.45 keV by a double crystal monochromator [Si (111), $\Delta E/E = 2 \times 10^{-4}$] served as the probe. The x-ray focal spot size was about 0.1 mm^2, i.e., considerably smaller than that of the laser to ensure that over the entire probed area the pump conditions were the same. The signal diffracted from the GaSb/InAs 002 planes ($\theta_{\text{Bragg}} = 7.1\,^\circ$) was recorded by an ultrafast streak camera [17] equipped with a CsI transmission photocathode. For readout the camera's phosphor screen was fiber optically coupled to an image intensifier and a charge-coupled device (CCD) camera. The laser operated at a repetition rate of 900 Hz and was synchronized to the storage ring clock and thus to the electron bunches with a jitter less than 10 ps by an adaptive oscillator cavity length. Since temporal resolution was achieved by the detector and not by the pulse length of the probe (the x-ray pulse from a single electron bunch was about 100 ps long), this jitter was not limiting the temporal resolution. For a reasonable S/N ratio, the signal of the order of 10^5 shots had to be accumulated. This made the jitter of the streak camera trigger relative to the laser pump the limiting factor for the temporal resolution of the whole setup. By triggering the streak camera with the laser itself using a low capacity photoconductive switch, an effective temporal resolution of the order of a picosecond was achieved. The streak camera itself had a single-shot temporal resolution of 500 fs and thus was not a limiting factor.

Figures 1 and 2 show measured and simulated evolution of the normalized 002-Bragg reflectivity $R(\theta, t)/R_0(\theta)$ (R_0: reflectivity of heterostructure before laser pump) of the laser heated GaSb/InAs MQW at two different x-ray energies, $E_1 = 16.37$ keV and $E_2 = 16.49$ keV, corresponding to two different locations on the rocking curve. The patterns are considerably different from the very periodic and rather slowly developing pattern from a laser excited bulk crystal [11,14], which is shown in the inset. This is a direct consequence of phonon branch folding. Phonon modes are excited not only in the longitudinal acoustic branch but also in the upper branches created by the folding process. It is the superposition of these modes, with equal wave vectors but different frequencies, which leads to the observed irregular fluctuations. This is shown in a more quantitative way in Fig. 3 where a Fourier based power spectrum estimate (PSE) [18] of the measured signal in Fig. 2 is presented. One can clearly see two peaks. The noise level can be inferred from the PSE of the signal without pump. The peak frequencies match those given for the probed phonon wave vector in the dispersion diagram in Fig. 4. Obviously, the higher frequency belongs to the back-folded branch. This is clear evidence for branch folding. Very recently another TRXD study of coherent phonons in a periodic heterostructure has been published [19]. However, the evolution of the x-ray reflectivity there

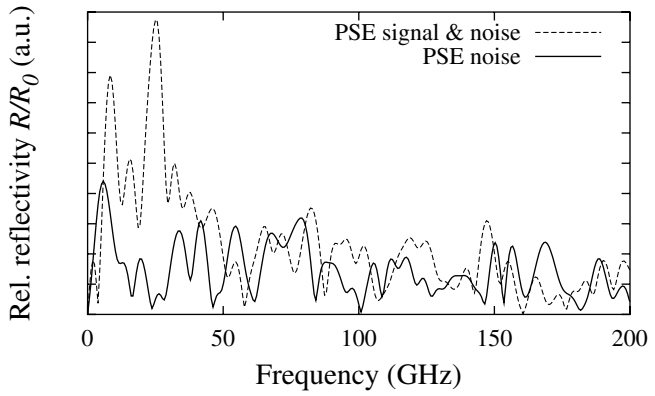

FIG. 3. Fourier based power spectrum estimate for the evolution of the normalized reflectivity at $\theta = \theta_{\text{Bragg}} + 0.61$ mrad with and without laser pump.

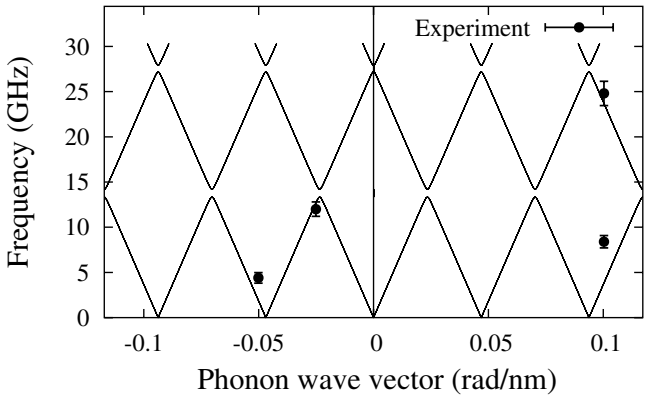

FIG. 4. Phonon dispersion diagram for the GaSb/InAs heterostructure (lines) calculated within an elastic continuum model [4]. Also shown are the experimentally observed frequencies [bullets, PSE of the recorded reflectivity $R(t)/R_0$]. The error bars represent the maximum error estimates of the error in the time calibration (linear regression) of the streak camera.

is of a single frequency and thus only a single phonon branch can be involved.

The choice of phonon wave vectors in Fig. 4 was dictated by the source limited S/N ratio. The diffracted x-ray intensity is highest and thus the S/N ratio best near the reduced BZ centers where the superlattice diffraction peaks are located. The data point at $q = -0.025$ rad/nm is an exception. The good S/N ratio there is due to the proximity to the central Bragg peak.

TRXD supplies more than just phonon wave vectors and frequencies: in principle, the laser inflicted transient strain can be reconstructed *ab initio* from the recorded signal of a single rocking curve, $R(\theta, t)$. However, the brightness of presently available x-ray sources is only sufficient to probe the region close to the center of the rocking curve where the reflectivity is high. Thus, so far only the BZ center is accessible. Therefore, the detection of phonons via TRXD is still somewhat model dependent. The simulated curves in Figs. 1 and 2 were created using an elastic continuum model for the generation and propagation of coherent acoustic phonons in a heterostructure [8]. The model uses a transfer matrix method to propagate laser field and elastic strain through the heterostructure. This method takes account for multiple reflections at the layer interfaces. In the case of the elastic strain, this procedure leads to two different kinds of modes: bulk and surface modes. The bulk modes correspond to the freely propagating longitudinal acoustic modes in a bulk crystal. Surface modes, on the other hand, remain at the surface. In the dispersion diagram, the latter are located in the small frequency gaps at the BZ boundary. A condition for the existence of longitudinal surface modes is that the acoustic impedance of the surface layer is smaller than that of the layer below. This condition is not fulfilled in the case of the GaSb/InAs MQW, since the acoustic impedance of the GaSb surface layer is larger than that of InAs. Thus, there are no surface modes in this experiment. Finally the x-ray reflectivity was modeled within the statistical dynamical theory of x-ray diffraction for dislocational mosaic crystals [20].

The match between measured and modeled x-ray reflectivity (Figs. 1 and 2, solid and dashed curves) is very good considering the low photon number and thereby limited S/N ratio. It should be noted that there is no free scaling factor for the normalized reflectivity R/R_0. To achieve this match it was necessary to adapt the model for the coherent phonon generation. It turned out that the strain profile predicted using interband absorption alone is too shallow. For comparison, the modeled time-dependent x-ray reflectivity based on plain interband absorption, too, is given in Figs. 1 and 2 (dotted curves). This can be explained by the self-modulation of the real and imaginary part of the refractive index due to the massive photogeneration of free carriers [21]. This effect was integrated into the model in the form of a first order approximation: it was assumed that the effective absorption coefficient increases linearly with the laser fluence $w(z, t)$, which at a given time t has passed through a layer at depth z, i.e., $\mu(z, t) = \mu_0 + 2\alpha w(z, t)$, where μ_0 stands for the interband absorption coefficient. The constant α was used as a free parameter to fit the modeled data to the experimental results. The simulated curves in Figs. 1 and 2 were generated with $\alpha = 3500$ m/J.

In earlier TRXD experiments with bulk crystals [15], the opposite effect was observed: the strain profiles were flatter than expected from plain interband absorption. This was explained by ambipolar diffusion. Following a steep density gradient, photogenerated electron-hole pairs diffuse into the bulk of the crystal. The electron-hole pairs carry and finally transfer their energy to the lattice beyond the laser absorption depth. In our experiment, these effects are not present due to the relative alignment of the valence and conduction bands of GaSb and InAs. In the GaSb/InAs heterojunction, the lower edge of the InAs conduction band lies about 100 meV below the upper edge of the GaSb valence band (so-called ''type-II broken-gap'') [22]. As a consequence, the electrons in the InAs conduction band and the holes in the GaSb valence band are confined between the forbidden zones of the respective neighbor layers. Thus, ambipolar diffusion across the interfaces is strongly inhibited.

This experiment has demonstrated the particular strengths of time-resolved x-ray diffraction (TRXD): it simultaneously provides information about phonon wavelengths, phonon frequencies, and the related atomic motion in real time. In contrast, optical methods require poorly known entities such as photoelastic constants or Raman tensors in order to interpret the results. Furthermore, x rays have large absorption depths in all materials allowing for deeper probing. This can be used, for example, to avoid surface effects or to probe layers buried under a thick cap

layer. In principle, the whole Brillouin zone (BZ) can be probed using x rays. The present limitation of TRXD to the BZ center is a purely technological one in contrast to the fundamental limitation of methods employing radiation in the visible range. With the advent of 4th generation x-ray sources [23,24], the technological limitation of insufficient brightness will be removed soon. TRXD is a powerful tool for studying the structural dynamics in a wide range of materials as shown here by the visualization of the dynamics in semiconductor heterostructures.

We would like to thank Nigel Mason for the preparation of the samples and Alexander Babkevich for his help with the x-ray diffractometer. This work was supported by the European commission through the Human Potential Program, the Swedish Science Foundation, and the Swedish Foundation for Strategic Research.

*Electronic address: peter.sondhauss@fysik.lth.se
URL: http://www-atom.fysik.lth.se/txrd
†A. Plech's present address: Department of Physics, University of Constance, D78457 Konstanz, Germany.

[1] P. Gross, V. Ramakrishna, E. Vilallonga, H. Rabitz, M. Littman, S. A. Lyon, and M. Shayegan, Phys. Rev. B **49**, 11100 (1994).
[2] N. Bonadeo, J. Erland, D. Gammon, D. Park, D. Katzer, and D. Steel, Science **282**, 1473 (1998).
[3] U. Özgür, C. W. Lee, and H. O. Everitt, Phys. Rev. Lett. **86**, 5604 (2001).
[4] S. M. Rytov, Akust. Zh. **2**, 71 (1956) [Sov. Phys. Acoust. **2**, 68 (1956)].
[5] C. Colvard, R. Merlin, M. V. Klein, and A. C. Gossard, Phys. Rev. Lett. **45**, 298 (1980).
[6] C. Colvard, T. A. Gant, M. V. Klein, R. Merlin, R. Fischer, H. Morkoc, and A. C. Gossard, Phys. Rev. B **31**, 2080 (1985).
[7] D. J. Lockwood, M. W. C. Dharma-wardana, J. M. Baribeau, and D. C. Houghton, Phys. Rev. B **35**, 2243 (1987).
[8] H. T. Grahn, H. J. Maris, J. Tauc, and B. Abeles, Phys. Rev. B **38**, 6066 (1988).
[9] N. W. Pu and J. Bokor, Phys. Rev. Lett. **91**, 076101 (2003).
[10] C. Rose-Petruck, R. Jimenez, T. Guo, A. Cavalleri, C. Siders, F. Ráski, J. Squier, B. Walker, K. Wilson, and C. Barty, Nature (London) **398**, 310 (1999).
[11] A. Lindenberg, I. Kang, S. Johnson, T. Missalla, P. Heimann, Z. Chang, J. Larsson, P. Bucksbaum, H. Kapteyn, H. Padmore *et al.*, Phys. Rev. Lett. **84**, 111 (2000).
[12] D. Reis, M. DeCamp, P. Bucksbaum, R. Clarke, E. Dufresne, M. Hertlein, R. Merlin, R. Falcone, H. Kapteyn, M. Murnane *et al.*, Phys. Rev. Lett. **86**, 3072 (2001).
[13] K. Sokolowski-Tinten, C. Blome, C. Dietrich, A. Tarasevitch, M. Horn von Hoegen, D. von der Linde, A. Cavalleri, J. Squier, and M. Kammler, Phys. Rev. Lett. **87**, 225701 (2001).
[14] J. Larsson, A. Allen, P. Bucksbaum, R. Falcone, A. Lindenberg, G. Naylor, T. Missalla, D. Reis, K. Scheidt, A. Sjörgen *et al.*, Appl. Phys. A **75**, 467 (2002).
[15] M. DeCamp, D. Reis, A. Cavalieri, P. Bucksbaum, R. Clarke, R. Merlin, E. Dufresne, D. Arms, A. Lindenberg, A. MacPhee *et al.*, Phys. Rev. Lett. **91**, 165502 (2003).
[16] R. Beanland, D. Dunstan, and P. Goodhew, Adv. Phys. **45**, 87 (1996).
[17] G. A. Naylor, K. Scheidt, J. Larsson, M. Wulff, and J. M. Filhol, Meas. Sci. Technol. **12**, 1858 (2001).
[18] W. Press, S. Teukolsky, W. Vetterling, and B. Flannery, *Numerical Recipes in C: The Art of Scientific Computing* (Cambridge University Press, Cambridge, England, 1992), 2nd ed..
[19] M. Bargheer, N. Zharvoronkov, Y. Gritsai, J. Woo, D. Kim, M. Woerner, and T. Elsaesser, Science **306**, 1771 (2004).
[20] V. A. Bushuev, Kristallografiya **34**, 279 (1989) [Sov. Phys. Crystallogr. **34**, 163 (1989)].
[21] D. Hulin, M. Combescot, J. Bok, A. Migus, J. Y. Vinet, and A. Antonetti, Phys. Rev. Lett. **52**, 1998 (1984).
[22] I. Vurgaftman, J. Meyer, and L. Ram-Mohan, J. Appl. Phys. **89**, 5815 (2001).
[23] J. Arthur, Rev. Sci. Instrum. **73**, 1393 (2002).
[24] B. Wiik, Nucl. Instrum. Methods Phys. Res., Sect. A **398**, 1 (1997).